International Journal of Modern Manufacturing Technologies
ISSN 2067–3604, Vol. XVI, No. 1 / 2024
https://doi.org/ 10.54684/ijmmt.2024.16.1.101

OPTIMIZING THE GEOMETRICAL PARAMETERS OF 3D PRINTED NEGATIVE STIFFNESS METAMATERIAL USING TAGUCHI METHOD

Sandip Patel, Harshit Dave

Sardar Vallabhbhai National Institute of Technology, Department of Mechanical Engineering
Surat 395007, India

Corresponding author: Harshit Dave, harshitkumar@yahoo.com

Abstract: The field of negative stiffness metamaterials (NSM) is a rapidly developing area within the realm of mechanical metamaterials. This work presents a novel negative stiffness metamaterial based on a bistable structure that consists of a straight beam with an elastic element shaped like a ring. Further, this work presents the findings of a Taguchi-based experiment aimed at optimizing geometrical parameters in negative stiffness metamaterial. The Taguchi method, known for its efficiency in experimental design and analysis, was employed to systematically study the effects of various factors on snapping force for a novel structure exhibiting negative stiffness. The experiment utilized L_{18} mixed level orthogonal array. All the test samples were fabricated using additive manufacturing technique. Signal-to-noise ratio analysis and analysis of variance were two statistical approaches that were used to comprehensively evaluate the acquired data. The results of this study provide valuable insights into the optimal geometrical configuration for maximizing snapping force of negative stiffness metamaterial.

Key words: Negative stiffness metamaterial, mechanical metamaterial, additive manufacturing, Taguchi method, ANOVA

1. INTRODUCTION

Mechanical metamaterials have emerged in recent years as a possible path for designing materials with unexpected characteristics not seen in nature [1–3]. These novel materials have exceptional mechanical capabilities that frequently contradict conventional material behaviour. Negative stiffness (NS) is one of these extraordinary properties. It has attracted a lot of interest because of its potential to create novel capabilities in a variety of engineering applications. The concept of negative stiffness challenges the conventional notion of stiffness as a measure of a material's resistance to deformation. Positive stiffness occurs when a material or structure experiences an increase in restoring force with increasing deformation. In contrast, with negative stiffness a material or structure experiences a decrease in restoring force with increasing deformation. This distinct behaviour results from the design of mechanical metamaterials, which use geometric arrangements to create negative effective stiffness over certain ranges of deformation.

The negative stiffness effect seen in Negative Stiffness Metamaterials (NSM) is typically accomplished by the use of elastic instability, notably snap-through buckling. The most common design technique for NSM is to incorporate a snapping mechanism, which is often based on curved beam [4–6] or straight beam [7–9] designs. The overall attributes of these NSM can be modified by properly tuning the topological and geometrical parameters, depending on the desired application [10–12]. Typically, NSM performance is affected by many geometrical parameters. This makes geometrical optimisation expensive as it involves large number of experiments. Previous researches have shown that complete factorial parametric studies for NSM are often carried out using FEA or analytical approaches, with experimental methods utilised to validate them [13–15]. A bistable NSM having unique geometry is describes in this paper. A patent application is submitted with the Indian Patent Office for this purpose [16].

Furthermore, this study employed the Taguchi experimental design approach. With its systematic method to effectively explore the parameter space and determine the ideal combination of parameters, the Taguchi experimental design technique has become an effective tool for optimizing geometrical designs in recent years [17–19]. The advantages of using this strategy include: i. the capacity to conduct robust experimentation with a small number of trials; ii. providing useful insights into the impacts of individual parameters and their combinations; and iii. assuring robust and dependable results.

2. MATERIALS AND METHODS

2.1. Geometrical Design

This work presents a novel bistable structure that consists of a straight beam with an elastic element shaped like a ring in the middle. The geometry and notations for this NS beam are depicted in Figure 1. Consistent out-of-plane thickness *t* characterises the rectangular cross section of the NS beam. L_0 represents the undeformed length of the NS beam. The schematic of fundamental bi-stable structure that illustrate its planner mechanism is depicted in Figure 2(a). Two identical NS beams are arranged in a V-configuration, with each beam having two pinned joints that allow for a single degree of rotation at both ends. Pinned joints at vertex of V-configuration are attached to moving support and the other to fixed support. This results in a balanced structure, allowing movable support to have a single degree of freedom of movement along a vertical linear path. When the moving support is at the extreme ends of its linear trajectory, the bistable mechanism has two stable states, labelled as I and III. NS beams are unstressed mechanically in these stable equilibrium states. Generally speaking, a bistable NS beam with the ring-shaped deflection element shown here is characterised as a pinned-guided beam that is substantially free to deflect between two stable positions when a sufficient force is applied at a point along the moving support. Thus, an elastic instability brought on by the ring-shaped element's deflection when force is applied along the moving support is main cause to achieve the NS effect.

The unique shape of the ring segment allows the pined-guided beam to bounce back and flex laterally while snapping between two stable positions. The in-plane width of ring segment $b(\beta)$ is functionally varying and it is function of *e*, *a*, and β. Where *e* represents the eccentricity of the ring segment's inner radius R_i and outer radius R_o with respect to its mean radius *R*, which is primarily responsible for the change in width of the ring segment. While, *a* is a non-negative constant responsible for minimum uniform width of the ring segment. The α denotes half angle of ring segment and β is the azimuth angle. The *c* denotes half opening of ring segment, which imparts geometrical constrains in maximum axial deformation of the pined-guided beam, within elastic limit of constitutive material. The following equations defines relation between geometrical parameters of ring segment.

$$R_i = R - (e + a) \tag{1}$$

$$R_o = R + (e + a) \tag{2}$$

$$b(\beta) = \sqrt{8e^2 + 4a^2 + 8e^2\cos\beta + 8ea\,(1 + \cos\beta)} \tag{3}$$

$$c = R\sin\alpha \tag{4}$$

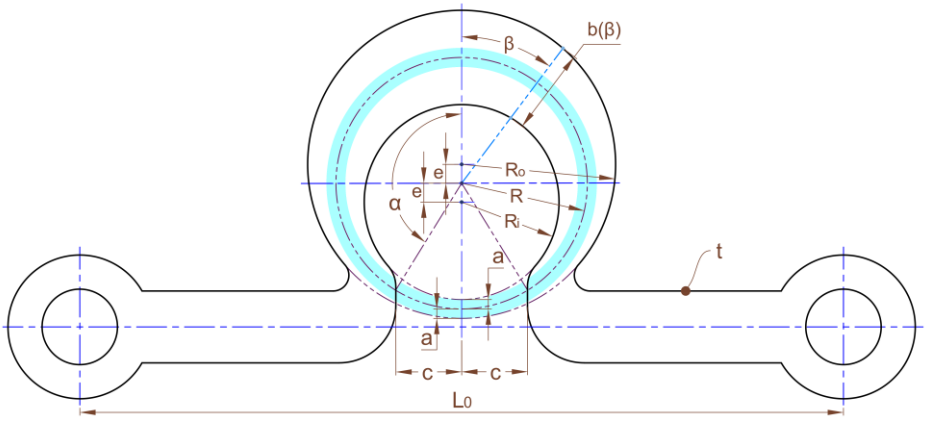

Fig. 1. The geometry and notations for the NS beam

The force-displacement behaviour of this bi-stable structure is illustrated in Figure 2(b). Initially, the force increases as displacement increases until it reaches to ultimate value of force F_{max}. Following then, the slop of the curve became negative, indicating negative stiffness. The bi-stable structure has two stable equilibrium conditions, illustrated by position I and III, with local minimum potential energy as depicted in Figure 2(b-c).

2.2 Materials and Additive Manufacturing

Initially, the CAD models of NSM are prepared in Solidworks software from Dassault Systemes and then imported into STEP file format. The STEP file format was chosen because it retains a high level of geometric accuracy, particularly when compared to STL file [20]. These STEP files are loaded into PrusaSlicer 2.6.1 from Prusa Research and turned into G-code files, which contain printing instructions for a 3D printer to build an object. Fused Deposition Modeling (FDM) process of additive manufacturing (AM) is used to create all the specimens for experimentation. 3D printing is carried out using a Prusa i3 MK3S bear upgrade printer (3DPrintronics, India). PLA+ filament (Numakers Asia LLP, India) of 1.75 diameter is used for 3D printing of specimens. It has beneficial qualities when compared to other FDM compatible thermoplastics, such as low cost, higher toughness, higher tensile strength, good layer adhesion, good geometrical accuracy, and ease of printing [21]. This makes it the most preferred material for FDM printers. The mechanical properties of PLA+ as supplied by manufacturer are as follows: density = 1.24 g/cc, tensile strength = 50 MPa, tensile modulus = 2315 MPa, flexural strength = 126 MPa, and flexural modulus = 4357 MPa. Blue PLA+ filament is used for NS beams, while white PLA+ filament is used for moving and fixed frame of specimens. The characteristic printing parameters for 3D printing of specimens are listed in Table 1.

Table 1. FDM printing process parameters

Parameter	Value
Nozzle diameter	0.4 mm
Extrusion temperature	210°
Build platform temperature	60°
Infill density	100%
Layer thickness	0.1 mm (0.2 mm for first layer)
Print speed	40 mm/s (20 mm/s for first layer)

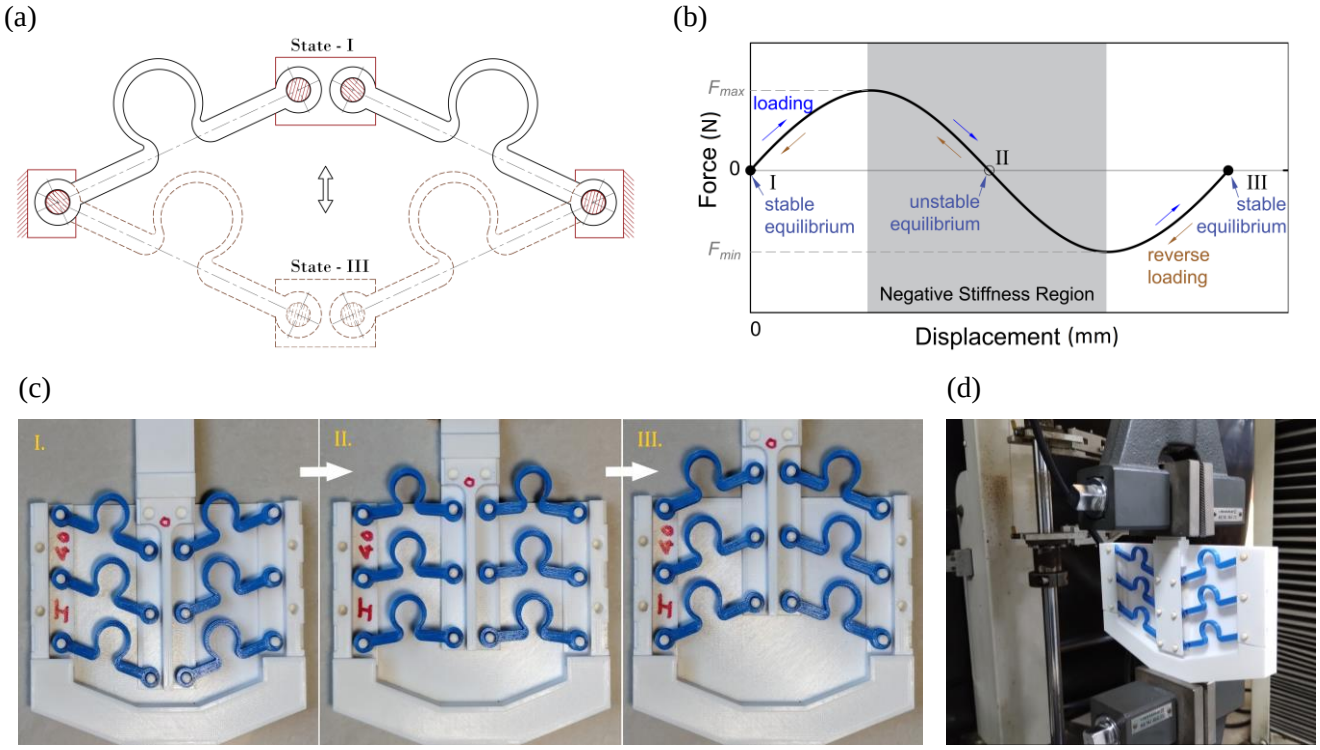

Fig. 2. For bi-stable NSM structure depicting its, (a) planner mechanism, (b) force-displacement behaviour, (3) 3D printed specimen having three parallel pairs of NS beams, and (d) experimental setup

2.3 Testing

Uniaxial tensile loading experiments were performed to determine the load-displacement curve for NSM snap-through transitions. NSM test specimens with three parallel pairs of NS beams organised in a V-configuration are created, as depicted in Figure 2(c). The six NS beams were manually assembled with a stationary support frame and a moving support frame for each sample. All the pinned joints are lubricated with oil to reduce effects of

friction and hysteresis. AG-IS Shimadzu universal testing machine is used to conduct Uniaxial tensile testing. The NSM's fixed support frame is clamped with the bottom fixed crosshead, while the moving support frame is clamped with the top moveable crosshead, as depicted in Figure 2(d). Quasi-static loading conditions were applied using a loading rate of 20 mm/min in a displacement control manner until the next stable configuration of NSM.

2.4 Taguchi Experimental Design

The Taguchi Method assists in identifying the optimal combination of control factors that give the required performance while minimising variability by methodically altering factors at different levels and effectively designing trials using orthogonal arrays. The Taguchi technique is used in this study primarily because of its capacity to efficiently explore a broad design space and discover the most critical parameters influencing performance while running tests with a limited number of trials.

Table 2. Design factors and their levels for Taguchi analysis of NS beam

Factors	Parameters	Notations & Units	Levels		
			1	2	3
A	length of NS beam	L_0 (mm)	40	60	-
B	NS beam thickness	t (mm)	4	5	6
C	ring thickness constant	a (mm)	0.3	0.4	0.5
D	ring eccentricity	e (mm)	0.3	0.4	0.5
E	half angle of ring	α (degree)	130	140	150

Table 3. L_{18} ($2^1 \times 3^4$) mixed level orthogonal array for experimentations

Experiment No.	Factors (Coded)					Factors (Uncoded)				
	A	B	C	D	E	L_0 (mm)	t (mm)	a (mm)	e (mm)	α (degree)
1	1	1	1	1	1	40	4	0.3	0.3	130
2	1	1	2	2	2	40	4	0.4	0.4	140
3	1	1	3	3	3	40	4	0.5	0.5	150
4	1	2	1	1	2	40	5	0.3	0.3	140
5	1	2	2	2	3	40	5	0.4	0.4	150
6	1	2	3	3	1	40	5	0.5	0.5	130
7	1	3	1	2	1	40	6	0.3	0.4	130
8	1	3	2	3	2	40	6	0.4	0.5	140
9	1	3	3	1	3	40	6	0.5	0.3	150
10	2	1	1	3	3	60	4	0.3	0.5	150
11	2	1	2	1	1	60	4	0.4	0.3	130
12	2	1	3	2	2	60	4	0.5	0.4	140
13	2	2	1	2	3	60	5	0.3	0.4	150
14	2	2	2	3	1	60	5	0.4	0.5	130
15	2	2	3	1	2	60	5	0.5	0.3	140
16	2	3	1	3	2	60	6	0.3	0.5	140
17	2	3	2	1	3	60	6	0.4	0.3	150
18	2	3	3	2	1	60	6	0.5	0.4	130

The goal of this study is to identify optimal combination of geometrical parameters to improve snapping force of NS beam i.e. F_{max}. The beam length L_0, and geometry of the ring segment are main factor affecting the snapping force. Based on geometrical relations define in section 2.1, the minimum set of parameters drive the ring geometry are t, a, e, R and α. Design factors and their levels for Taguchi analysis of NS beam are listed in Table 2. In addition, the NS beam is arranged in a V-configuration at an angle of 20° from the horizontal. While, the mean radius R is kept 7 mm. L_{18} mixed level orthogonal array is used for experiment design, with one factor at level two and four factors at level three (Table 3). To confirm that the results are repeatable, each experiment was done twice, for a total of 36 test runs.

3. RESULTS AND DISCUSSION

The experiment results were recorded in terms of force-displacement, as shown in Figure 3. The Taguchi technique was used to implement the experimental design, which was run with Minitab software version 20.3. The maximum snapping force F_{max} is derived from these results as a response factor. The Taguchi method based experiments yielded important insights into how geometrical parameters affects maximum snapping force F_{max}. The collected data were thoroughly analysed using statistical techniques including signal-to-noise (S/N) ratio analysis and analysis of variance (ANOVA). The S/N ratio analysis is used for the determination of optimal levels for the geometrical parameters under consideration. While, ANOVA is performed to assess the contribution of each parameter and identify the most influential parameters.

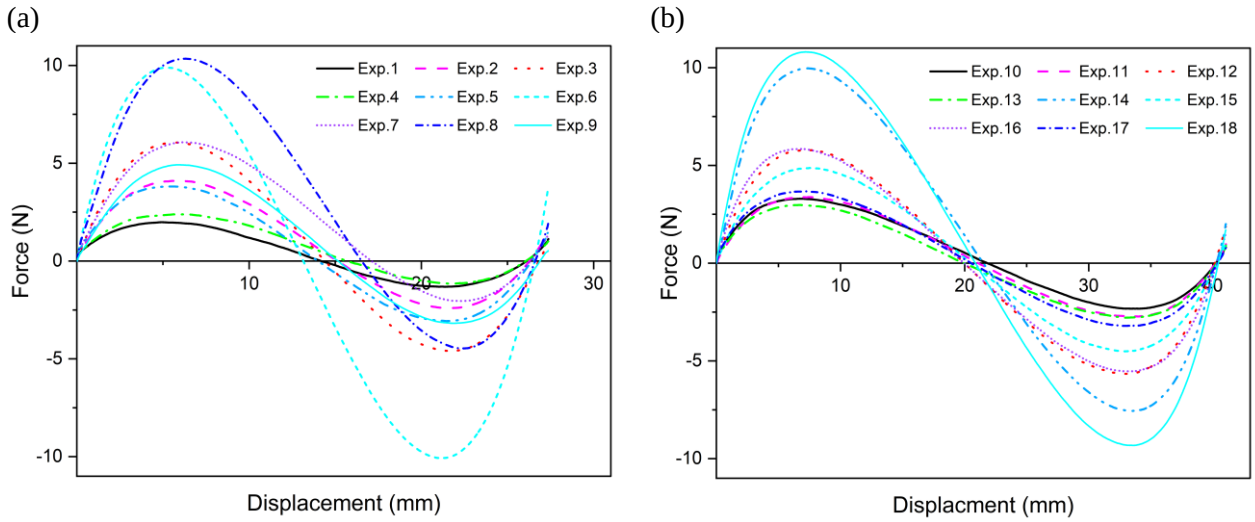

Fig. 3. Force-displacement curves for experiment: (a) 1 to 9, and (b) 10 to 18

Table 4. Response table for signal to noise ratios (larger is better)

Level	**A**	**B**	**C**	**D**	**E**
1	13.97	12.09	11.21	10.90	**15.73**
2	**14.40**	14.08	14.64	14.52	14.36
3		**16.39**	**16.72**	**17.14**	12.48
Delta	0.43	4.30	5.51	6.24	3.25
Rank	5	3	2	1	4

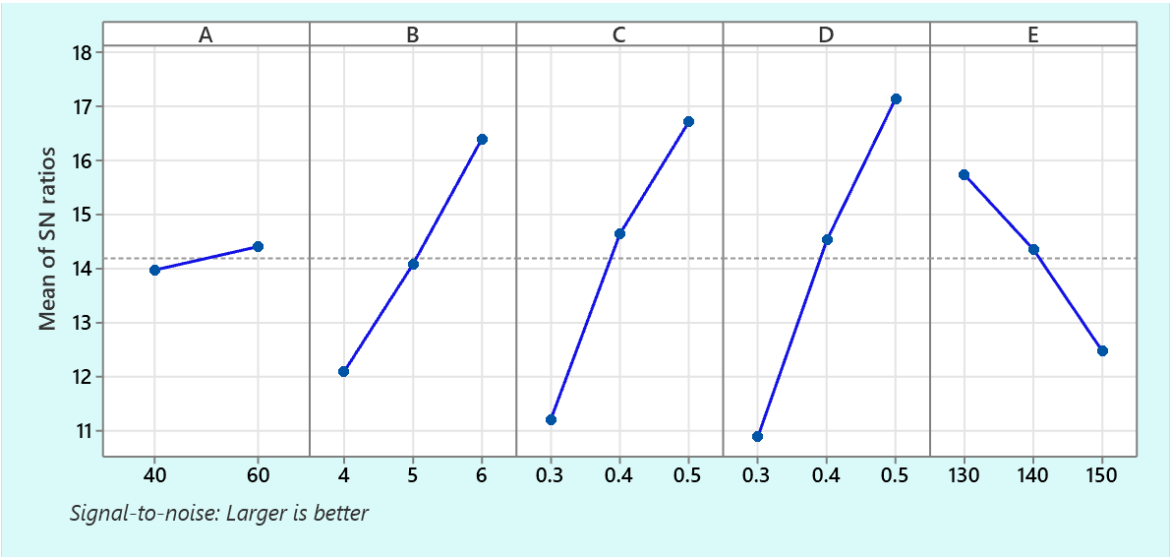

Fig. 4. Main effects plot for signal-to-noise ratios

It is desirable to achieve higher snapping force to improve negative stiffness performance of NSM. To maximise the snapping force F_{max} in S/N ratio analysis, the "larger is better" approach is employed. Figure 4 displays the graphs of the mean values of the S/N ratios that have been plotted for each process parameter. Table 4 presents a summary of the mean S/N ratios measured for each level of input parameters. Wherein, the optimal level of each parameter for maximum snapping force F_{max} is highlighted in bold. Accordingly, the best combination for key factors is: NS beam length of the 2nd level, NS beam thickness of the 3rd level, ring thickness constant of the 3rd level, ring eccentricity of the 3rd level, and ring half angle of the 1st level, i.e L_0 = 60 mm, t = 6 mm, a = 0.5 mm, e = 0.5 mm, and α = 130°. The results show that the D-C-B-E-A order is the rank of the influencing degree of the factors on the maximum snapping force. That means ring eccentricity e and ring thickness constant a are first and second most influencing parameters, respectively.

The statistical outcomes for response variable using ANOVA are presented in Table 5. The analysis performed is precise, with R-squared values of 98% (Table 6) and the residual error of 2%, indicating that the chosen model is a good match. The findings are regarded statistically significant when the P-value are less than 0.005 and the F-value are the highest. Based on P-value, it is observed that parameters t, a, e and α are statistically significant to increase maximum snapping force F_{max}. Whereas contribution of L_0 is much lesser that is 0.27%.

Table 5. Analysis of Variance (ANOVA)

Source	DoF	Seq SS	Contribution	Adj SS	Adj MS	F-Value	P-Value
L_0 (mm)	1	0.01111	0.27%	0.01111	0.01111	1.1	0.32568
t (mm)	2	0.73645	18.19%	0.73645	0.36822	36.32	0.00010
a (mm)	2	1.23088	30.41%	1.23088	0.61544	60.71	0.00001
e (mm)	2	1.56415	38.64%	1.56415	0.78207	77.14	0.00001
α (degree)	2	0.42455	10.49%	0.42455	0.21227	20.94	0.00066
Error	8	0.08110	2.00%	0.08110	0.01014		
Total	17	4.04824	100.00%				

Table 6. ANOVA model summary for maximum snapping force

S	R-sq	R-sq(adj)	PRESS	R-sq(pred)
0.100687	98.00%	95.74%	0.410581	89.86%

4. CONCLUSIONS

The Taguchi-based experiment on geometrical optimization presented in this research paper offers valuable insights into the geometrical design and improvement of the NSM. By systematically varying geometrical parameters and employing robust experimental techniques, key factors influencing system performance were identified, and optimal parameter settings were determined. Furthermore, the experiment's results contribute to a deeper understanding of the interaction effects among different geometrical parameters, providing valuable knowledge for future design iterations and optimization efforts. The key findings of this study are as follows:

- According to the Taguchi method, the optimum geometrical parameters for maximum snapping force F_{max} is achieved when L_0 = 60 mm, t = 6 mm, a = 0.5 mm, e = 0.5 mm, and α = 130°.
- The rank of the influencing degree of the factors on the maximum snapping force found from S/N ratio analysis and ANOVA are same and in decreasing order of influence it is e - a - t - α - L_0.
- Length of the NS beam does not have any significant effect on the maximum snapping force of NSM.
- The geometrical parameters responsible for ring geometry, that includes t, a, e and α, are most influencing parameters on the maximum snapping force of NSM.

In conclusion, the Taguchi-based experiment proved to be effective in optimizing geometrical parameters for improving the performance of NSM. The insights gained from this experiment pave the way for further research and practical applications in field of mechanical metamaterials requiring geometrical optimization.

Conflicts of Interest: There is no conflict of interest.

REFERENCES

1. Zadpoor, A. A., (2016). *Mechanical meta-materials*, Mater. Horiz., 3, 371-381.
2. Surjadi, J. U.; Gao, L.; Du, H.; Li, X.; Xiong, X.; Fang, N.X.; Lu, Y., (2019). *Mechanical Metamaterials and Their Engineering Applications*, Adv. Eng. Mater., 21, 1800864.

3. Fan, J.; Zhang, L.; Wei, S.; Zhang, Z.; Choi, S. K.; Song, B.; Shi, Y., (2021). *A review of additive manufacturing of metamaterials and developing trends*, Materials Today, 50, 303–328.
4. Chen, S.; Tan, X.; Hu, J.; Zhu, S.; Wang, B.; Wang, L.; Jin, Y.; Wu, L., (2021). *A novel gradient negative stiffness honeycomb for recoverable energy absorption*, Compos B Eng., 215, 108745.
5. Zhang, Y.; Tichem, M.; van Keulen, F., (2021). *A novel design of multi-stable metastructures for energy dissipation*, Mater Des., 212, 110234.
6. Li, Q.; Yang, D.; Ren, C.; Mao, X, (2022). *A systematic group of multidirectional buckling-based negative stiffness metamaterials*, Int J Mech Sci. 232, 107611.
7. Ha, C. S.; Lakes, R. S.; Plesha, M. E., (2018). *Design, fabrication, and analysis of lattice exhibiting energy absorption via snap-through behavior*, Mater Des., 141, 426–437.
8. Meng, Z.; Liu, M.; Zhang, Y.; Chen, C. Q., (2020). *Multi-step deformation mechanical metamaterials*, J. Mech. Phys. Solids., 144, 104095.
9. Hou, Z.; Duan, C.; Yu, Y.; Wang, Z., (2023). *Reusable and efficient energy-absorbing architected materials via synergy of snap-through instability and inter-locking mechanism*, Extreme Mech Lett., 58, 101948.
10. Restrepo, D.; Mankame, N. D.; Zavattieri, P. D., (2015). *Phase transforming cellular materials*, Extreme Mech. Lett., 4, 52–60.
11. Yang, H.; Ma, L., (2018). *Multi-stable mechanical metamaterials by elastic buckling instability*, J. Mater. Sci., 54, 3509–3526.
12. Chen, B.; Chen, L.; Du, B.; Liu, H.; Li, W.; Fang, D., (2021). *Novel multifunctional negative stiffness mechanical metamaterial structure: Tailored functions of multi-stable and compressive mono-stable*, Compos B Eng., 204, 108501.
13. Wu, L.; Xi, X.; Li, B.; Zhou, J., (2017). M*ulti-Stable Mechanical Structural Materials*, Adv. Eng. Mater., 20, 1700599.
14. Tan, X.; Wang, B.; Wang, L.; Zhu, S.; Chen, S.; Yao, K.; Xu, P., (2022). *Effect of beam configuration on its multistable and negative stiffness properties*, Compos Struct., 286, 115308.
15. Tan, X.; Li, Y.; Wang, L.; Yao, K.; Ji, Q.; Wang, B.; Laude, V.; Kadic, M., (2023). *Bioinspired Flexible and Programmable Negative Stiffness Mechanical Metamaterials*, Advanced Intelligent Systems, 5.
16. Dave, H.; Patel, S.; Desai, K.: (2024). *Multi-stable negative stiffness structure and mechanical logic gates*, Indian Patent Application no. 202421004116.
17. Radhakrishnan, J.; Sridhar, S.; Zuber, M.; Ng, E.Y.K.; B., S.S., (2023). *Design optimization of a Contra-Rotating VAWT: A comprehensive study using Taguchi method and CFD*, Energy Convers Manag., 298, 117766.
18. Usta, F.; Zhang, Z.; Kurtaran, H.; Scarpa, F.; Türkmen, H.S.; Mecitoğlu, Z., (2022). *Design optimization of modified re-entrant auxetic metamaterials reinforced with asymmetric edge cells for crushing behavior using the Taguchi method*, Journal of the Brazilian Society of Mechanical Sciences and Engineering, 44, 395.
19. Crnjac, M.; Aljinovic, A.; Gjeldum, N.; Mladineo, M., (2019). *Two-stage product design selection by using PROMETHEE and Taguchi method: A case study*, Advances in Production Engineering & Management, 14, 39–50.
20. Qin, Y.; Qi, Q.; Scott, P.J.; Jiang, X., (2019). *Status, comparison, and future of the representations of additive manufacturing data. Computer-Aided Design*, 111, 44–64.
21. Dave, H. K.; Patel, S. T., (2021). *Introduction to Fused Deposition Modeling Based 3D Printing Process*, Fused Deposition Modeling Based 3D Printing, Dave, H.K., Davim, J.P. (Ed(s)), pp. 1-21, Springer, Cham.

Received: April 10th, 2024 / Accepted: June 15th, 2024 / Paper available online: June 20, 2024